Emerging Infectious Diseases Core Facility Platform
NDMC, Taiwan.

Test Report

Report No: EID/202209-A01 Date: 2022-09-29

Testing Period: 2022.07.01~09.29

The following test samples are provided and confirmed by the supplier:

Request partner: AINOS INC. TAIWAN BRANCH (USA)

Testing purpose: To evaluate the efficacy of antiviral drugs against SARS-CoV-2 in hamsters-continuous daily dosing test.

Precautions:

- The content of this report is only responsible for the samples provided by AINOS INC. TAIWAN BRANCH (USA)
- Any modification of original data in this report is invalid.
- Application of this test report is invalid without agreement from Emerging Infectious Diseases Core Facility Platform, NDMC, Taiwan.
- The document number of Memorandum of understanding between National Defense Medical College and AINOS INC. TAIWAN BRANCH (USA) is「國醫衛勤字第 1110066192 號」.

Jyh-Hwa Kau 2022-09-29

Jyh-Hwa Kau Date

Principal Investigator

Emerging Infectious Diseases Core Facility Platform,

National Defense Medical Center, Taipei, Taiwan

Evaluation of the efficacy of antiviral drugs against SARS-CoV-2 in hamsters-continuous daily dosing test

Test Report

Core facility platform for emerging infectious disease research,
National Defense Medical College, Taiwan

September 29, 2022

Test term: July 1, 2022~ September 29, 2022

Catalogue

1. Abstract

This case evaluated the efficacy of antiviral drugs against SARS-CoV-2 in hamsters. The oral mucosal drugs, VELDONA®, used as antiviral drugs were provided by AINOS INC. TAIWAN BRANCH (USA). Hamsters were sacrificed and virus load was determined by both RT-qPCR and $TCID_{50}$. Body weight daily was measured during the experiment period.

2. Study outline

2.1. Animals: Hamsters; 26 per study depending on extent of sampling

2.2. Age at challenge: ~5-6 weeks

2.3. Challenge: Intranasal (50ul/nare)

2.4. Challenge Dose: $1x10^5$ pfu/ml SARS-CoV-2

2.5. Challenge strain: SARS-CoV-2 (Omicron variant)

3. Materials and Methods

3.1. Cell line and virus

Vero E6 cells were cultured in DMEM medium with 10% fetal bovine serum. Cell passage numbers in all cases were less than 25. SARS-CoV-2 virus was provided by Taiwan Center for Disease Control (hCoV-19/Taiwan/IPM-63/2022; EPI_ISL_12097305) and amplified in Vero E6 cells. SARS-CoV-2 titers were determined via plaque assays and processed in BSL-3 or BSL-4 laboratories.

3.2. Quantitative real-time RT-PCR (RT-qPCR) assays

100 μL of tissues supernatant was taken for RNA extraction via TANBead Nucleic Acid Extraction kit. After RNA being quantified, 1 μg of RNA was reverse transcribed to cDNA using SuperScript IV Reverse Transcriptase kit (Invitrogen). Subsequently, RT-qPCR was performed with a PowerTrack SYBR Green Master Mix ((Applied biosystems) and the LightCycler 480 system using primer pairs specific for the NP gene. GAPDH was used as the internal control.

3.2.1. PCR primer sequences and reaction setup

We searched the published literature and found the primers targeting GAPDH, SARS-CoV-2 NP gene that can be used in SYBR Green based quantitative PCR assay.

The following primers were used for Q-PCR assay in this test.

Gene	Primer Name	Sequence
SARS CoV2_NP	SARSCoV2_QPCR_F	GCCTCTTCTCGTTCCTCATCAC
	SARSCoV2_QPCR_R	AGCAGCATCACCGCCATTG
GAPDH	Hamster_G3pdhQPCR_F	GACATCAAGAAGGTGGTGAAGC
	Hamster_G3pdhQPCR_R	CATCAAAGGTGGAAGAGTGGGA

3.2.2. PCR reaction setup

(1) Pre-incubation

Target (°C)	Mode Acquisition	(hh:mm:ss) Hold	(°C/s) Ramp Rate	(°C) Sec Target	(°C) Step size	(cycles) Step Delay
50	None	00:02:00	2.20	0	0	0
95	None	00:02:00	4.40	0	0	0

(2)Amplification (40 cyclers)

Target (°C)	Mode Acquisition	(hh:mm:ss) Hold	(°C/s) Ramp Rate	(°C) Sec Target	(°C) Step size	(cycles) Step Delay
95	None	00:00:15	4.40	0	0	0
56	None	00:00:15	2.20	0	0	0
60	Single	00:00:40	4.40	0	0	0

3.3. Median tissue culture infectious dose ($TCID_{50}$) assay

Confluent Vero E6 cells on 96-well plates were incubated with 100 µL of serial 10-fold dilutions of virus in MEM containing 1% FBS for 1 h at 37°C. Next, the virus was removed from the 96-well plates and 100 µL of fresh MEM with 1% FBS was added to the cells. After the change of medium, cells infected with SARS-CoV-2 underwent a 5-day incubation period with SARS-CoV and the cytopathic effect was recorded via crystal violet staining. Median tissue culture infectious dose ($TCID_{50}$) was determined by the Reed and Muench method.

3.4. Pathological section and interpretation of lung tissue

Entrust the National Laboratory Animal Center to perform HE staining and interpretation of lung tissue pathological sections. The histopathological evaluation was performed on the submitted lungs. Severity of lesions (except inflammation area of the lung) was graded according to the methods described by Shackelford et al. (Toxicologic Pathology, Vol 30, No 1, pp93-96, 2002). Degrees of lesions were graded histopathologically from zero to five depending on severity (0 = not present; 1 = minimal (< 1%); 2 = slight (1–25%); 3 = moderate (26–50%); 4 =moderately severe (51–75%); 5 = severe/high (76–100%)).

4. Animal experiments

4.1. Ethics Statement

Male golden hamsters were obtained from the National Laboratory Animal Center (National Applied Research Laboratories, Taiwan). All experiments were performed at the ABSL-3 core facility, (Institute of Preventive Medicine, National Defense Medical College). The hamsters were randomized from different litters into experimental groups and were acclimatized at the ABSL-3 facility for one week before the experiments. The study protocol was reviewed and approved by the Committee on the Institutional Animal Care and Use, Institute of Preventive Medicine (Permit number:AN-111-24).

4.2. Test drugs

4.2.1. One test drug (VELDONA®) and dilution buffer (Placebo) were provided by AINOS INC. TAIWAN BRANCH (USA).

4.2.2. For VELDONA®: According to our previous preventive and/or therapeutic results of influenza studies (effective and toxicity does on mice), the converted effective dose for hamster is [redacted]U/ 100g (QD), and no toxicity is found. After deducting the overlapping part, we suggest test dose for the hamster study is above.

4.2.3. For Placebo: Dilution buffer

4.3. For Administration:

VELDONA® is diluted and dissolved to [redacted] IU/ μl in dilution buffer, and aliquots were stored at 4°C until use. Un-anaesthetized mice are administered the VELDONA® (use [redacted] IU/ 100g) or dilution buffer by the sublingual route, hamsters were held in the intraperitoneal (ip) injection position and administered directly under the tongue using a micropipette.

Table 1. The design of VELDONA® for COVID-19 antiviral efficacy study in hamsters (1)

Group[a]	Treatment [b]	Schedule	Route	Dose Level	Animal No. [c]
1-1/1-2/1-3	Placebo	QD	sublingual	0	4/4/4
2-1/2-2/2-3	VELDONA®	QD	sublingual	[redacted] IU/dose [redacted] IU/100g)	5/5/4

[a] Animals in groups 1-1/2-1 will be sacrificed on Day 2, in group 1-2/2-2 on Day 5, and in group 1-3/2-3 on Day 10 for various analysis

[b] Placebo group 1 (1-1～1-3) of 12 mice are received 10 ul of dilution buffer through mucosal route and served as control. Test group 2 (2-1～2-3) of 14 mice are administered VELDONA® daily for 5 days prior to virus infection and a further 10 days after virus infection on Day 0. Mice number in different subgroups

[c] Mice number in different subgroups

Table 2. The design of VELDONA® for COVID-19 antiviral efficacy study in hamsters (2)

Study Day	Treatment		Challenge (intranasal)	Body Weight	Nasal turbinates for virus titer	Lung examination for virus titer and pathological section	Serum collection
	Group 1	Group 2	Group 1-2				
-5	V			V			
-4	V			V			
-3	V			V			
-2	V			V			
-1	V			V			
0	V		V	V			
1	V			V			
2	V			V	V	V	V
3	V			V			
4	V			V			
5	V			V	V	V	V
6	V			V			
7	V			V			
8	V			V			
9	V			V			
10	V			V	V	V	V

One left lobe for pathological section, right 4 lobes for viral titer and qPCR

4.4. SARS-CoV-2 challenge

All male golden hamsters at 5-6 weeks old were fed adaptively one week before the beginning of the experiment on day zero. According to hamsters body weight, administration of the test drugs was performed via grouping plan. One hour later, all hamsters were anesthetized and inoculated by the intranasal (IN) route with 100 µL ($1x10^5$ PFU/mL) of SARS-CoV-2 virus.

4.5. Sample Collection and Processing:

4.5.1. Viral titer determination (Nasal turbinates/Lung)

4.5.1.1. Tissues (Nasal turbinates ; Lung right lobes) will be placed in an empty tube for homogenization for viral qPCR (NP plus GAPDH genes).

4.5.1.2. Tissues (Lung right lobes) will be placed in an empty tube for homogenization for live virus $TCID_{50}$ by Vero cell culture.

4.5.1.3. Others stored at -80°C for further study.

4.5.2. Lung pathology examination

Tissues (from left lobe) will be harvested in cassette for histopathology H&E stain.

4.5.3. Serum collection

Samples will be collected and stored at -80°C for further study.

4.6. Lungs and nasal turbinates processing steps

Lung collection number and processing method were as shown in Figure 1. “Lung 1” was transferred to a 2 mL tube containing respectively 1 mL of DMEM medium and 3 mm glass beads. They were crushed using a Tissue Lyser machine (Bertin/Precellys 24). 100 µL supernatant media (Lung RT-qPCR supernatant) was transferred to a 2 mL tube containing 0.9 mL of TRIzol reagent for RNA extraction. 100 µL supernatant media were ready to perform plaque assay. Both 250 µL supernatant media were stored at −80 °C for backup. The extraction of nasal turbinates RT-qPCR supernatant were follow the procedure of lung tissue processing.

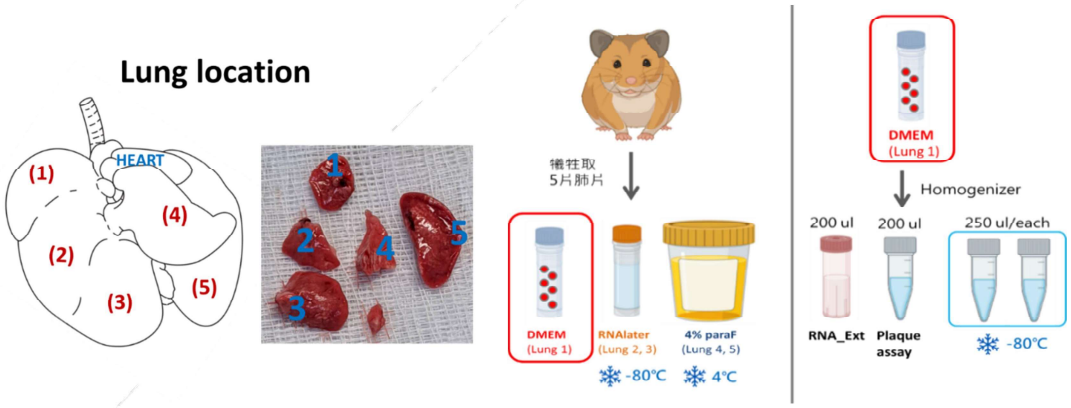

Figure 1. Schematic of lung collection number and processing methods

5. Results

5.1. Hamster body weight monitoring

Table 3. Raw data table of hamster body weight (g)

		11-Jul	12-Jul	13-Jul	14-Jul	15-Jul	16-Jul	17-Jul	18-Jul
Group	Item	Day-5	Day-4	Day-3	Day-2	Day-1	Day0	Day1	Day2
1-1	1A	[redacted]							
	1B	91.85	92.55	92.5	92.85	93.7	94.34	93.21	93.99
	1C	93.6	93.9	93.9	93.4	95.92	95.69	95.35	95.43
	1D	[redacted]							
1-2	1E	[redacted]							
	1F	[redacted]							
	1G	99.5	102.35	103.3	106.3	105.08	109.15	106.78	108.32
	1H	100.35	102.45	104.65	102.9	104.25	105.77	104.45	104.95
1-3	1M	97.85	97.65	98.85	101.45	101.27	101	100.79	101.31
	1N	97.35	96.9	98.65	101.85	101.47	102.22	99.53	102.02
	1O	[redacted]							
	1P	[redacted]							
2-1	2A	[redacted]							
	2B	108.35	106.35	107.35	110.65	109.79	109.09	109.05	109.58
	2C	107.25	106.6	107.6	107.9	109.91	110.31	109.11	111.1
	2D	[redacted]							
	2R	110.65	111.85	113.3	114.55	115.03	113.79	114.51	111.09
2-2	2E	105.6	106.9	107.35	109.45	109.14	108.84	109.64	111.11
	2F	103.35	108	108.8	111.35	111.27	111.41	111.26	114.27
	2G	104.05	107.6	110.1	110.45	112.07	111.97	111.04	111.88
	2H	[redacted]							
	2S	[redacted]							
2-3	2M	112.15	107.15	107.15	112.6	113.69	113.32	113.94	114.49
	2N	107.2	103.6	104.15	107.75	110.81	110.88	108.85	111.33
	2O	[redacted]							
	2P	[redacted]							

		19-Jul	20-Jul	21-Jul	22-Jul	23-Jul	24-Jul	25-Jul	26-Jul
Group	Item	Day3	Day4	Day5	Day6	Day7	Day8	Day9	Day10
1-1	1A								
	1B								
	1C								
	1D								
1-2	1E	103.07	104.06	105.72					
	1F	[redacted]							
	1G	[redacted]							
	1H	106	107.35	110.23					
1-3	1M	101.16	102.38	103.48	103.61	104.93	106.57	107.1	108.08
	1N	102.03	102.46	103.52	105.52	107.61	108.22	108.19	108.24
	1O	[redacted]							
	1P	[redacted]							
2-1	2A								
	2B								
	2C								
	2D								
	2R								
2-2	2E	111.41	112.41	112.23					
	2F	114.71	116.51	117.12					
	2G	[redacted]							
	2H	[redacted]							
	2S	121.67	123.06	123.66					
2-3	2M	114.94	118.04	117.24	117.21	118.33	118.77	119.63	120.66
	2N	[redacted]							
	2O	112.03	113.52	112.41	112.31	113.64	115.14	116.17	116.97
	2P	[redacted]							

5.2. Quantitative real-time RT-PCR (RT-qPCR) raw data in hamster tissues

Table 4. The viral load raw data table in hamster tissues

Group	Nasal turbinate samples	SARS_NP copies / 10^5 gapdh copies	Lung samples	SARS_NP copies / 10^5 gapdh copies
1-1	01_Day2_1A_N	[redacted]	27_Day2_1a_L	[redacted]
	02_Day2_1B_N	322747	28_Day2_1b_L	86917
	03_Day2_1C_N	186047	29_Day2_1c_L	ND
	04_Day2_1D_N	[redacted]	30_Day2_1d_L	ND
2-1	13_Day2_2A_N	[redacted]	39_Day2_2a_L	[redacted]
	14_Day2_2B_N	11439	40_Day2_2b_L	ND
	15_Day2_2C_N	[redacted]	41_Day2_2c_L	4973
	16_Day2_2D_N	47905	42_Day2_2d_L	[redacted]
	17_Day2_2R_N	882771	43_Day2_2e_L	ND
1-2	05_Day5_1E_N	186324	31_Day5_1e_L	ND
	06_Day5_1F_N	982011	32_Day5_1f_L	[redacted]
	07_Day5_1G_N	[redacted]	33_Day5_1g_L	ND
	08_Day5_1H_N	[redacted]	34_Day5_1h_L	[redacted]
2-2	18_Day5_2E_N	ND	44_Day5_2f_L	[redacted]
	19_Day5_2F_N	[redacted]	45_Day5_2g_L	[redacted]
	20_Day5_2G_N	[redacted]	46_Day5_2h_L	ND
	21_Day5_2H_N	316	47_Day5_2m_L	ND
	22_Day5_2S_N	15	48_Day5_2n_L	ND
1-3	09_Day10_1M_N	400	35_Day10_1m_L	[redacted]
	10_Day10_1N_N	[redacted]	36_Day10_1n_L	[redacted]
	11_Day10_1O_N	46	37_Day10_1o_L	ND
	12_Day10_1P_N	[redacted]	38_Day10_1p_L	ND
2-3	23_Day10_2M_N	34	49_Day10_2o_L	ND
	24_Day10_2N_N	[redacted]	50_Day10_2p_L	ND
	25_Day10_2O_N	[redacted]	51_Day10_2r_L	[redacted]
	26_Day10_2P_N	ND	52_Day10_2s_L	[redacted]

5.3. Plaque assay ($TCID_{50}$) of lung and nasal turbinates

Table 5. Raw data table of plaque assay ($TCID_{50}$)

Day of post inoculation	Group	Item	Lung ($TCID_{50}$/mL)
2	1-1	1A	3.16
		1B	4.57
		1C	[redacted]
		1D	[redacted]
	2-1	2A	[redacted]
		2B	2.14
		2C	[redacted]
		2D	[redacted]
		2R	3.16
5	1-2	1E	0
		1F	0
		1G	0
		1H	0
	2-2	2E	0
		2F	0
		2G	0
		2H	0
		2S	0
10	1-3	1M	0
		1N	0
		1O	0
		1P	0
	2-3	2M	0
		2N	0
		2O	0
		2P	0

5.4. Histopathological Examination

5.4.1. Information of Submitted Specimens

Paraformaldehyde-fixed left lobe of lungs from SARS-CoV-2 (Omichron variant) inoculated Syrian hamsters were submitted for histopathological examination. The information of submitted tissues was presented in the following table:

Groups	Treatment	Animal ID.	Day of post inoculation with SARS-CoV-2	Number of animals
1	SARS-CoV-2 only	1A, 1B, 1C, 1D	2	4
		1E, 1F, 1G, 1H	5	4
		1M, 1N, 1O, 1P	10	4
2	SARS-CoV-2 + Test article	2A, 2B, 2C, 2D, 2R	2	5
		2E, 2F, 2G, 2H, 2S	5	5
		2M, 2N, 2O, 2P	10	4

5.4.2. Histopathological Examination Results:

The microscopic alterations are presented in **Histopathology Finding Table**. The pathological photos are presented in **Figure 1~30.** Histologically, Syrian hamsters infected with SARS-CoV-2 (Omicron variant) presented lesions including:

Mixed-cellular inflammation, peribronchial infiltration, and perivascular infiltration

The lesions were characterized by a mixture of heterophils with lymphocytic and histiocytic cell types within alveoli/interstitial and peribrochial and perivascular in the lung. The lesion severity was minimal.

Bronchial epithelial cell degeneration/necrosis with or without inflammatory infiltration in bronchiole

The lesions were observed in lungs of SARS-CoV-2 inoculated animals and characterized by cellular swelling, cytoplasmic vacuolation, perinuclear clear spaces, pyknosis of nuclei of affected epithelium mixing up with heterophils infiltrate into the bronchial lumen. The lesion severity was minimal.

Vasculitis and endothelialitis

The lesions were observed in lungs of SARS-CoV-2 inoculated animals. Endothelialitis is characterized by blood vessel bulging into the lumen due to an infiltration by macrophages and lymphocytes. The lesion severity was minimal.

In addition, **osseous metaplasia in alveoli** and **alveolar mineralization** were observed in some submitted lungs. The lesion may be attributable to spontaneous or incidental lesion. Artificial injury related extravasated blood cells in alveolar lumina was considered as related to tissue sampling injury.

Comments:

1. In this study, mock group (no virus inoculated) did not submitted.

2. The SARS-CoV-2 inoculated related lesions including (1) Mixed-cellular inflammation, peribronchial infiltration, and perivascular infiltration; (2) Bronchial epithelial cell degeneration/necrosis with or without inflammatory infiltration in bronchiole; (3) Vasculitis and endothelialitis.

3. Under-inflation of the lung and erythrocytes filled of the alveoli (artificial finding) were observed in most submitted lungs, histopathological examination was limited by these artifacts.

5.4.3. Histopathology Finding

Table 6. Histopathology Finding Table under SARS-CoV-2 only treatment (1)

Group	**1**					
Treatment	**SARS-CoV-2 only**					
Animal ID.	**1A**	**1B**	**1C**	**1D**	**1E**	**1F**
Day of post inoculation	**2**	**2**	**2**	**2**	**5**	**5**
Number of examined lobe	**1**	**1**	**1**	**1**	**1**	**1**
Lung						
Under-inflation of the lung	+	+	+	+	+	0
Inflammation area of the lung: Mixed-cellular inflammation, peribronchial/perivascular infiltration	[redacted]					
Epithelial necrosis/degeneration with or without inflammatory cell infiltration of the bronchiole	0	0	0	0	0	0
Regenerative hyperplasia, bronchial epithelium	0	0	0	0	0	0
Foreign body in bronchiole	0	0	0	0	0	0
Alveolar wall necrosis	0	0	0	0	0	0
Hyperplasia of type II alveolar epithelial cells	0	0	0	0	0	0
Vasculitis and endothelialitis	0	0	1	1	1	0
Vascular thrombosis	0	0	0	0	0	0
Hemorrhage, alveoli and perivascular area	0	0	0	0	0	0
Edema, alveoli and perivascular area	0	0	0	0	0	0
Osseous metaplasia in alveoli	0	0	0	0	1	0
Alveolar mineralization	0	0	0	0	0	1
Pleural thickening	0	0	0	0	0	0
Artificial injury (extravasated blood cells in alveolar lumina, equipment injury)	+	+	+	+	+	+

+: Present

Degrees of other lesions (except inflammation area) were graded histopathologically From zero to five depending on severity (0 = not present; 1 = minimal (< 1%); 2 = slight (1–25%); 3 = moderate (26–50%); 4 = moderately severe (51–75%); 5 = severe/high (76–100%)).

Table 7. Histopathology Finding Table under SARS-CoV-2 only treatment (2)

Group	**1**					
Treatment	**SARS-CoV-2 only**					
Animal ID.	**1G**	**1H**	**1M**	**1N**	**1O**	**1P**
Day of post inoculation	**5**	**5**	**10**	**10**	**10**	**10**
Number of examined lobe	**1**	**1**	**1**	**1**	**1**	**1**
Lung						
Under-inflation of the lung	+	+			+	+
Inflammation area of the lung: Mixed-cellular inflammation, peribronchial/perivascular infiltration	[redacted]					
Epithelial necrosis/degeneration with or without inflammatory cell infiltration of the bronchiole	0	0	0	0	0	0
Regenerative hyperplasia, bronchial epithelium	0	0	0	0	0	0
Foreign body in bronchiole	0	0	0	0	0	0
Alveolar wall necrosis	0	0	0	0	0	0
Hyperplasia of type II alveolar epithelial cells	0	0	0	0	0	0
Vasculitis and endothelialitis	0	0	0	0	0	0
Vascular thrombosis	0	0	0	0	0	0
Hemorrhage, alveoli and perivascular area	0	0	0	0	0	0
Edema, alveoli and perivascular area	0	0	0	0	0	0
Osseous metaplasia in alveoli	0	0	0	0	0	0
Alveolar mineralization	0	0	0	0	0	0
Pleural thickening	0	0	0	0	0	0
Artificial injury (extravasated blood cells in alveolar lumina, equipment injury)	+	+	+	+	+	+

+: Present

Degrees of other lesions (except inflammation area) were graded histopathologically From zero to five depending on severity (0 = not present; 1 = minimal (< 1%); 2 = slight (1–25%); 3 = moderate (26–50%); 4 = moderately severe (51–75%); 5 = severe/high (76–100%)).

Table 8. Histopathology Finding Table under SARS-CoV-2+VELDONA® treatment (1)

Group	**2**						
Treatment	**SARS-CoV-2 + Test article**						
Animal ID.	**2A**	**2B**	**2C**	**2D**	**2R**	**2E**	**2F**
Day of post inoculation	**2**	**2**	**2**	**2**	**2**	**5**	**5**
Number of examined lobe	**1**	**1**	**1**	**1**	**1**	**1**	**1**
Lung							
Under-inflation of the lung	+	+	+	+	+	+	+
Inflammation area of the lung: Mixed-cellular inflammation, peribronchial/perivascular infiltration	[redacted]						
Epithelial necrosis/degeneration with or without inflammatory cell infiltration of the bronchiole	0	0	0	0	0	1	0
Regenerative hyperplasia, bronchial epithelium	0	0	0	0	0	0	0
Foreign body in bronchiole	0	0	0	0	0	0	0
Alveolar wall necrosis	0	0	0	0	0	0	0
Hyperplasia of type II alveolar epithelial cells	0	0	0	0	0	0	0
Vasculitis and endothelialitis	0	0	0	0	0	1	0
Vascular thrombosis	0	0	0	0	0	0	0
Hemorrhage, alveoli and perivascular area	0	0	0	0	0	0	0
Edema, alveoli and perivascular area	0	0	0	0	0	0	0
Osseous metaplasia in alveoli	0	0	0	0	0	0	0
Alveolar mineralization	0	0	0	0	0	0	0
Pleural thickening	0	0	0	0	0	0	0
Artificial injury (extravasated blood cells in alveolar lumina, equipment injury)	+	+	+	+	+	+	+

+: Present

Degrees of other lesions (except inflammation area) were graded histopathologically From zero to five depending on severity (0 = not present; 1 = minimal (< 1%); 2 = slight (1–25%); 3 = moderate (26–50%); 4 = moderately severe (51–75%); 5 = severe/high (76–100%)).

Table 9. Histopathology Finding Table under SARS-CoV-2+VELDONA® treatment (2)

Group	**2**						
Treatment	**SARS-CoV-2 + Test article**						
Animal ID.	**2G**	**2H**	**2S**	**2M**	**2N**	**2O**	**2P**
Day of post inoculation	**5**	**5**	**5**	**10**	**10**	**10**	**10**
Number of examined lobe	**1**	**1**	**1**	**1**	**1**	**1**	**1**
Lung							
Under-inflation of the lung	-	-	-	-	-	-	-
Inflammation area of the lung: Mixed-cellular inflammation, peribronchial/perivascular infiltration	[redacted]						
Epithelial necrosis/degeneration with or without inflammatory cell infiltration of the bronchiole	1	0	1	0	0	0	0
Regenerative hyperplasia, bronchial epithelium	0	0	0	0	0	0	0
Foreign body in bronchiole	0	0	0	0	0	0	0
Alveolar wall necrosis	0	0	0	0	0	0	0
Hyperplasia of type II alveolar epithelial cells	0	0	0	0	0	0	0
Vasculitis and endothclialitis	1	0	1	0	0	0	0
Vascular thrombosis	0	0	0	0	0	0	0
Hemorrhage, alveoli and perivascular area	0	0	0	0	0	0	0
Edema, alveoli and perivascular area	0	0	0	0	0	0	0
Osseous metaplasia in alveoli	0	0	0	0	0	0	0
Alveolar mineralization	0	0	0	1	0	0	0
Pleural thickening	0	0	0	0	0	0	0
Artificial injury (extravasated blood cells in alveolar lumina, equipment injury)	+	+	+	+	+	+	+

+: Present

Degrees of other lesions (except inflammation area) were graded histopathologically From zero to five depending on severity (0 = not present; 1 = minimal (< 1%); 2 = slight (1–25%); 3 = moderate (26–50%); 4 = moderately severe (51–75%); 5 = severe/high (76–100%)).

5.4.4. Photographs of Pathology Examination

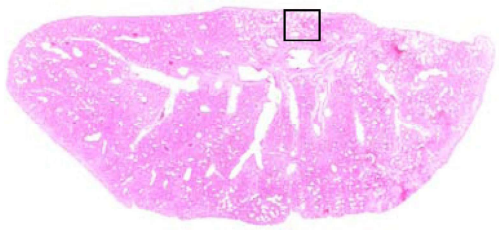

Fig. 1: 1A lung 12.5X, H&E
Under-inflation of the lung. Boxed area indicates in **Fig. 2**.

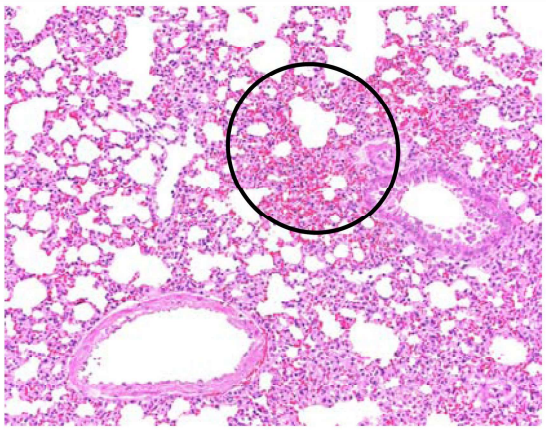

Fig. 2: 1A lung 200X, H&E
Artificial injury (extravasated blood cells in alveolar lumina, circle area). Higher magnification of **Fig. 1** boxed area.

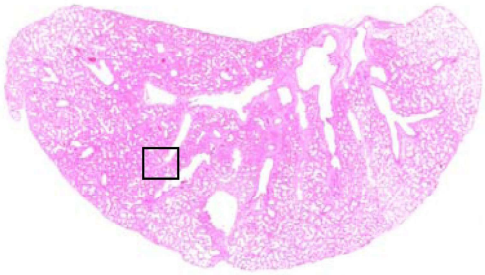

Fig. 3: 1C lung 12.5X, H&E
Under-inflation of the lung. Boxed area indicates in **Fig. 4**.

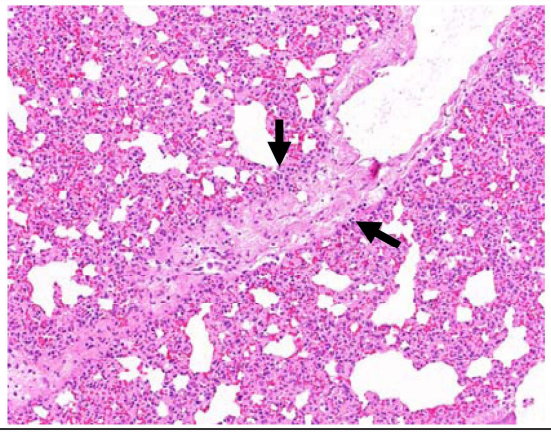

Fig. 4: 1C lung 200X, H&E
Perivascular mixed cell infiltration (arrows). Higher magnification of **Fig. 3** boxed area.

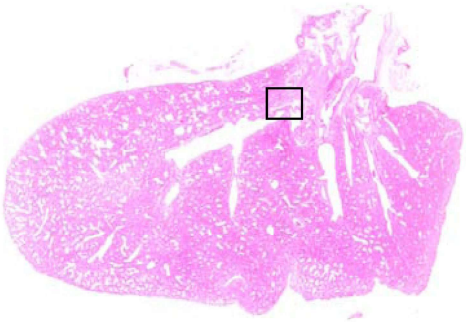

Fig. 5: 1E lung 12.5X, H&E
Under-inflation of the lung. Boxed area indicates in **Fig. 6**.

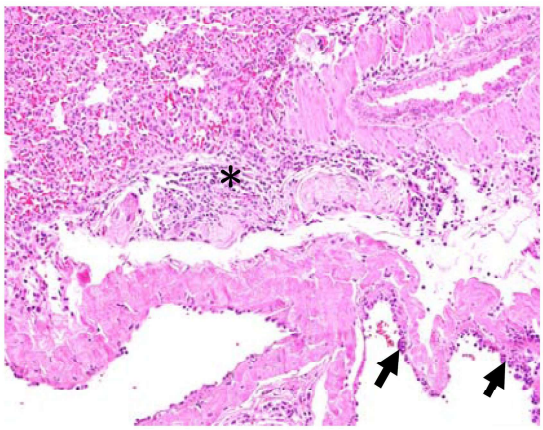

Fig. 6: 1E lung 200X, H&E
Perivascular mixed cell infiltration (*) and endothelialitis (arrows). Higher magnification of **Fig. 5** boxed area.

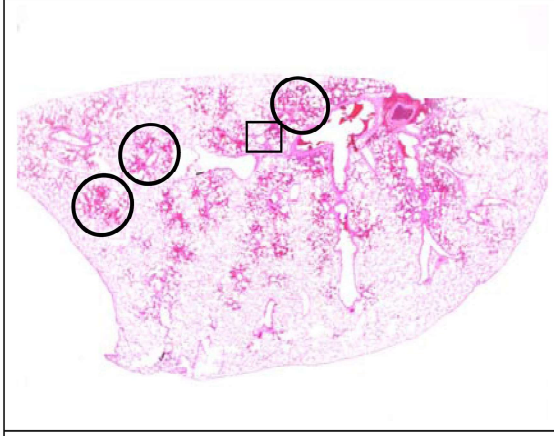

Fig. 7: 1F lung 12.5X, H&E
Artificial injury (extravasated blood cells in alveolar lumina, circle areas). Boxed area indicates in **Fig. 8**.

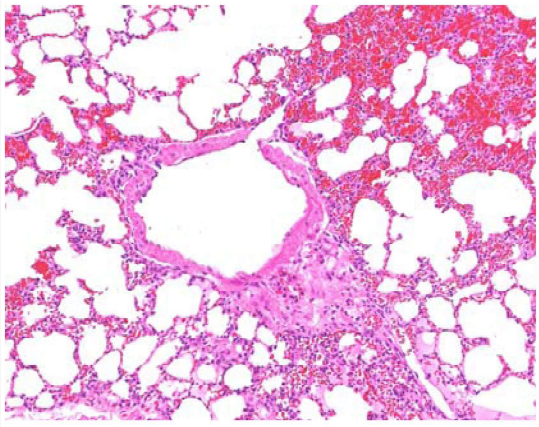

Fig. 8: 1F lung 200X, H&E
Perivascular mixed cell infiltration and extravasated blood cells in alveolar lumina. Higher magnification of **Fig. 7** boxed area.

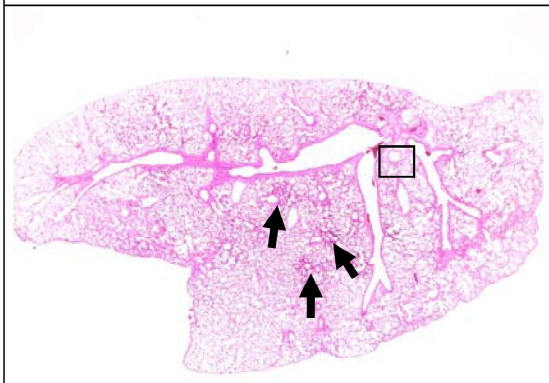

Fig. 9: 1M lung 12.5X, H&E
Artificial injury (extravasated blood cells in alveolar lumina, arrows). Boxed area indicates in **Fig. 10**.

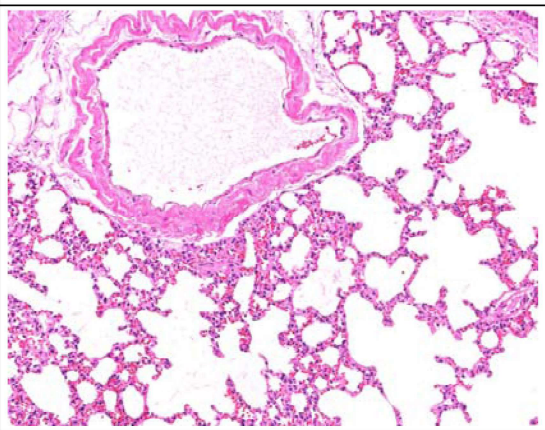

Fig. 10: 1M lung 200X, H&E
No significant lesions. Higher magnification of **Fig. 9** boxed area.

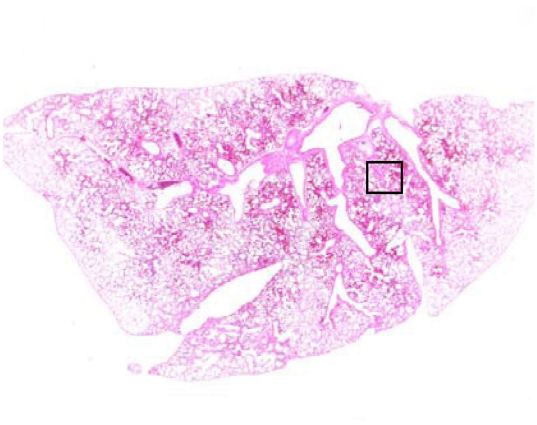

Fig. 11: 1N lung 12.5X, H&E
Artificial injury (extravasated blood cells in alveolar lumina). Boxed area indicates in **Fig. 12**.

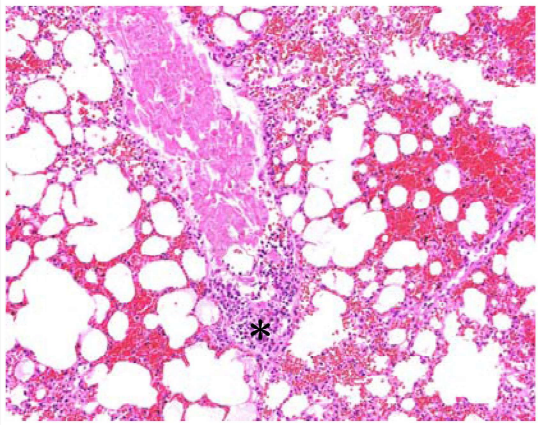

Fig. 12: 1N lung 200X, H&E
Perivascular mixed cell infiltration (∗) and extravasated blood cells in alveolar lumina. Higher magnification of **Fig. 11** boxed area.

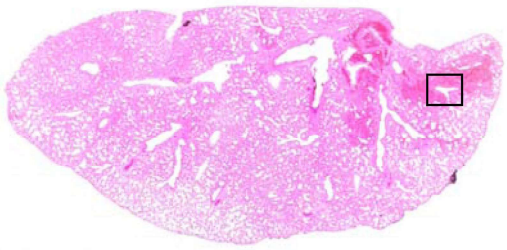

Fig. 13: 2A lung 12.5X, H&E
Under-inflation of the lung. Artificial injury (extravasated blood cells in alveolar lumina). Boxed area indicates in **Fig. 14**.

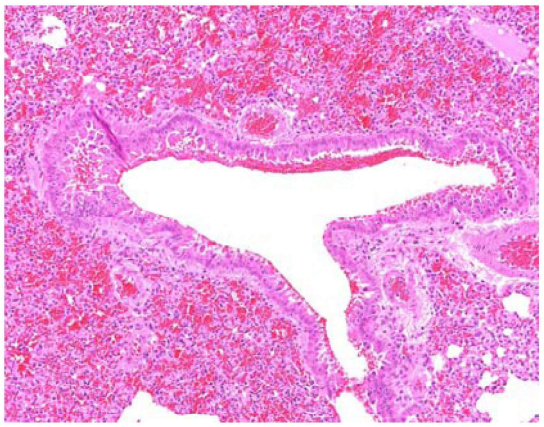

Fig. 14: 2A lung 200X, H&E
Artificial injury (extravasated blood cells in alveolar and bronchial lumina). Higher magnification of **Fig. 13** boxed area.

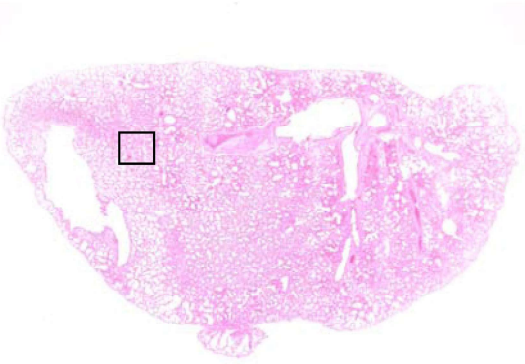

Fig. 15: 2C lung 12.5X, H&E
Under-inflation of the lung. Boxed area indicates in **Fig. 16**.

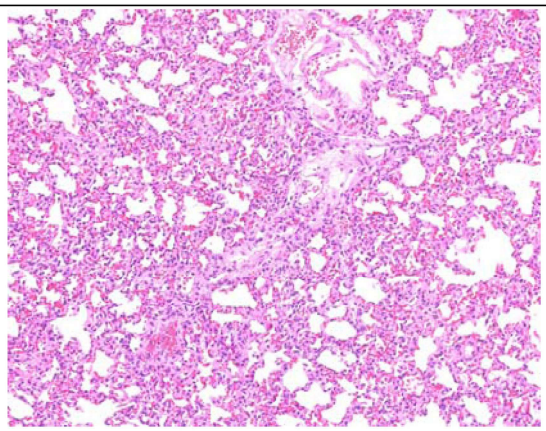

Fig. 16: 2C lung 200X, H&E
Perivascular mixed cell infiltration. Higher magnification of **Fig. 15** boxed area.

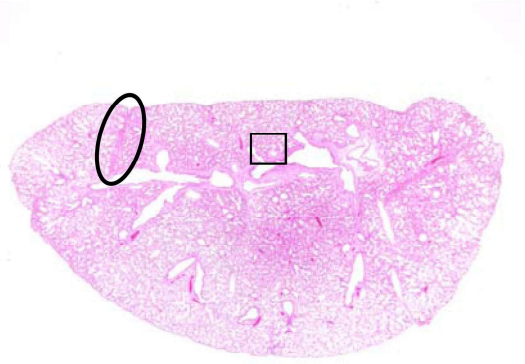

Fig. 17: 2E lung 12.5X, H&E
Artifact related to necropsy procedure (circle area). Boxed area indicates in **Fig. 18**.

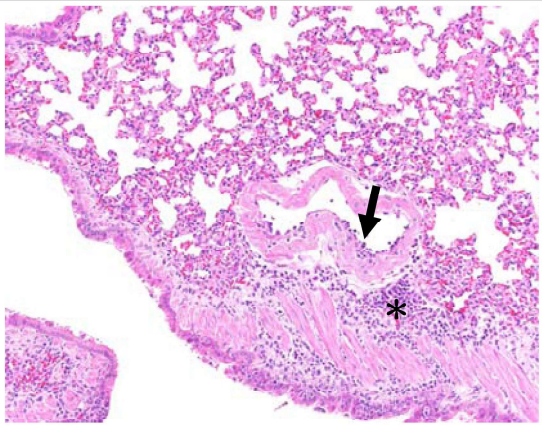

Fig. 18: 2E lung 200X, H&E
Perivascular mixed cell infiltration (*) and vasculitis (arrow). Higher magnification of **Fig. 17** boxed area.

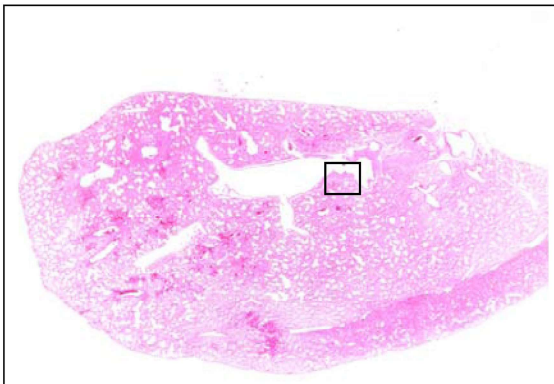

Fig. 19: 2S lung 12.5X, H&E
Artificial injury (extravasated blood cells in alveolar lumina). **Under-inflation of the lung.** Boxed area indicates in **Fig. 20**.

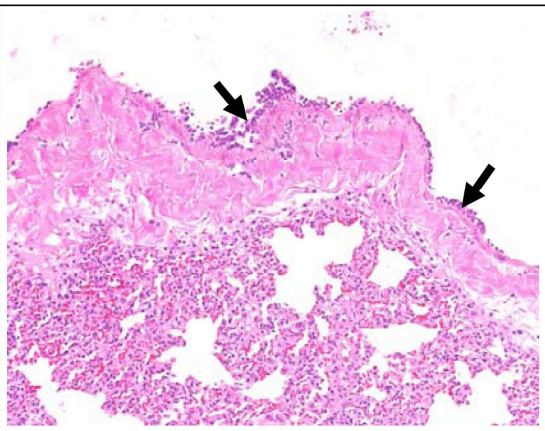

Fig. 20: 2S lung 200X, H&E
Endothelialitis (arrows).
Higher magnification of **Fig. 19** boxed area.

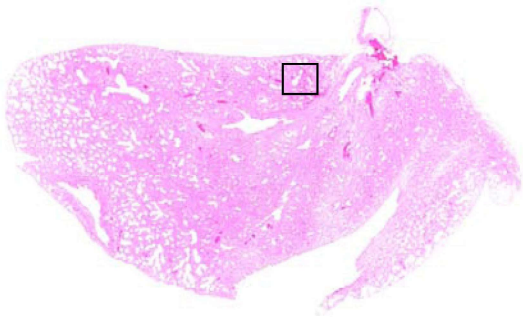

Fig. 21: 2M lung 12.5X, H&E
Under-inflation of the lung. Boxed area indicates in **Fig. 22**.

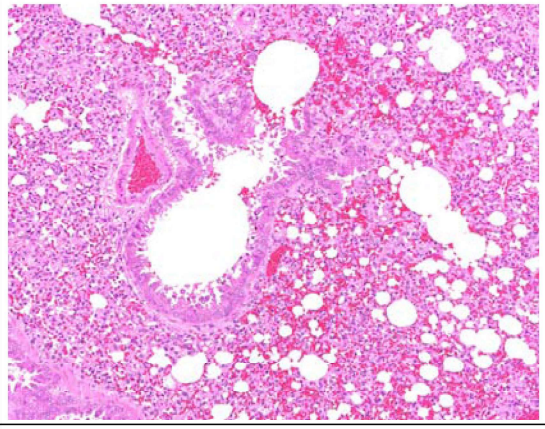

Fig. 22: 2M lung 400X, H&E
Artificial injury (extravasated blood cells in alveolar and bronchial lumina). Higher magnification of **Fig. 21** boxed area.

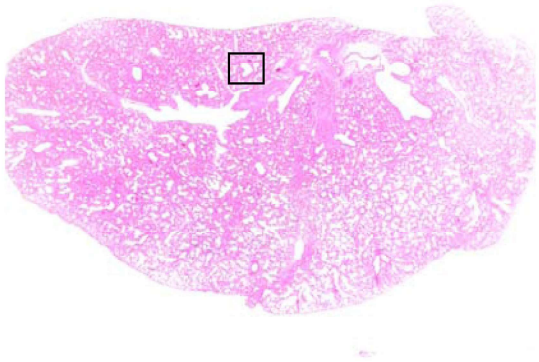

Fig. 23: 2N lung 12.5X, H&E
Under-inflation of the lung. Boxed area indicates in **Fig. 24**.

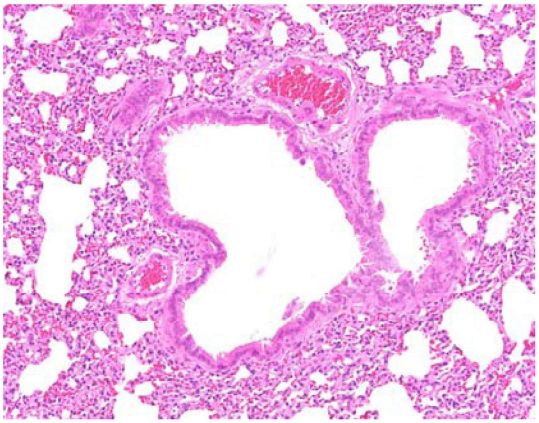

Fig. 24: 2N lung 400X, H&E
No significant lesions.
Higher magnification of **Fig. 23** boxed area.

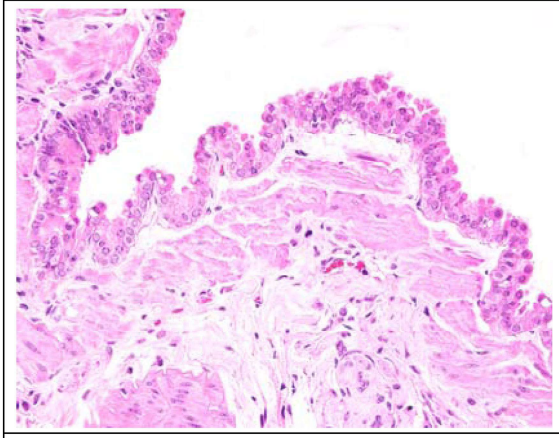

Fig. 25: 1A lung 400X, H&E
No significant lesions of bronchiolar epithelium.

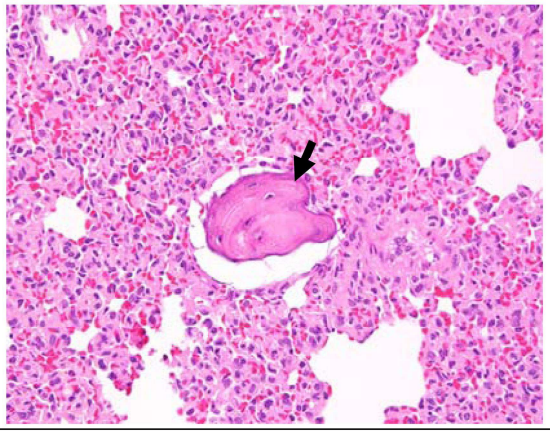

Fig. 26: 1E lung 400X, H&E
Osseous metaplasia in alveoli (arrow).

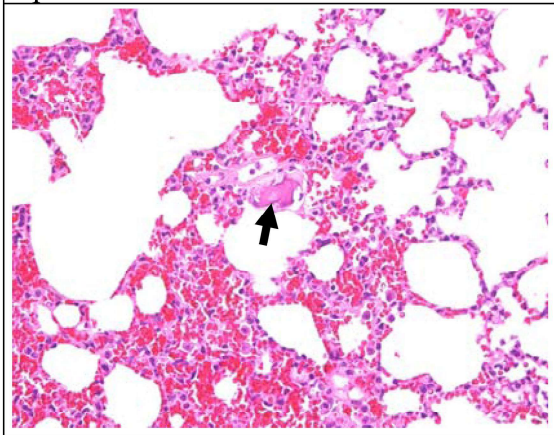

Fig. 27: 1F lung 400X, H&E
Alveolar mineralization (arrow).

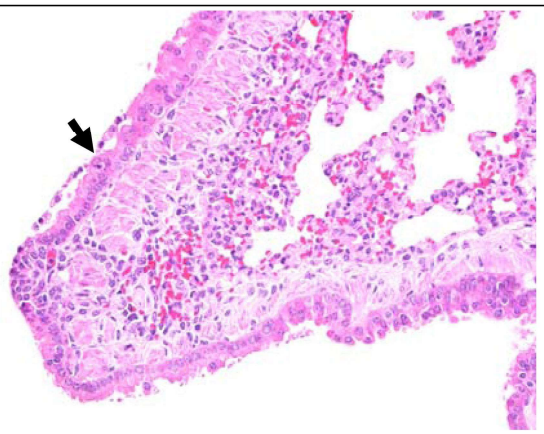

Fig. 28: 2E lung 400X, H&E
Bronchiolar epithelial degeneration/necrosis. Cell debris within the bronchiolar lumen (arrow).

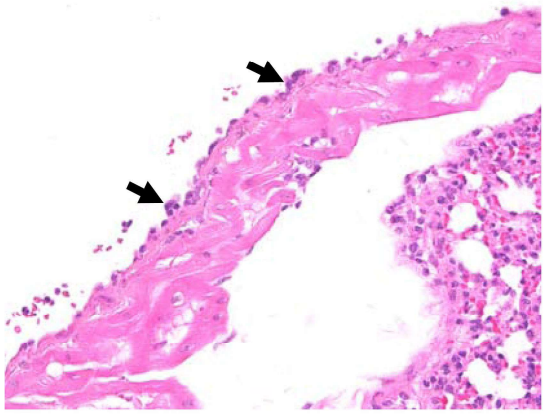

Fig. 29: 2G lung 400X, H&E
Endothelialitis (arrows).

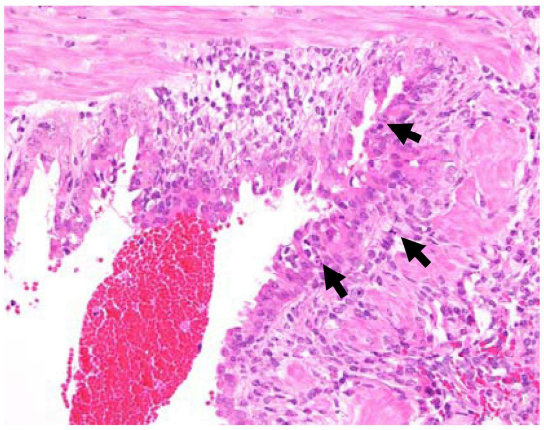

Fig. 30: 2S lung 400X, H&E
Bronchiolar epithelial degeneration/necrosis with inflammation (arrows).

6. Appendix

Original histopathological report from National Laboratory Animal Center in Taiwan.

7. References

[1] Wen-Fang Tang, Hui-Ping Tsai, Yu-Hsiu Chang, Tein-Yao Chang, Chung-Fan Hsieh, Chia-Yi Lin, Guan-Hua Lin, Yu-Li Chen, Jia-Rong Jheng , Ping- Cheng Liu, Chuen -Mi Yang, Yuan-Fan Chin, Cheng Cheung Chen, Jyh -Hwa Kau, Yi-Jen Hung, Po- Shiuan Hsieh, Jim-Tong Horng. Perilla (Perilla frutescens) leaf extract inhibits SARS-CoV-2 via direct virus inactivation. Biomedical Journal, 2021, https://doi.org/10.1016/j.bj.2021.01.005

[2] Driouich, JS., Cochin, M., Lingas, G. et al. Favipiravir antiviral efficacy against SARS-CoV-2 in a hamster model. Nat Commun 12, 1735 (2021).

[3] TOURET, F., GILLES, M., BARRAL, K., NOUGAIREDE, A., VAN HELDEN, J., DECROLY, E., DE LAMBALLERIE, X. & COUTARD, B. 2020. In vitro screening of a FDA approved chemical library reveals potential inhibitors of SARS-CoV-2 replication. Sci Rep, 10, 13093.

[4] Marinowic DR, Zanirati G, Rodrigues FVF, Grahl MVC, Alcara AM, Machado DC, Da Costa JC. 2021. A new SYBR Green real-time PCR to detect SARS-CoV-2. Sci Rep. Jan 26;11:2224.

[5] Ribeiro-Romao RP, Saavedra AF, Da-Cruz AM, Pinto EF, Moreira OC. 2016. Development of real-time PCR assays for evaluation of immune response and parasite load in golden hamster (Mesocricetus auratus) infected by Leishmania (Viannia) braziliensis. Parasit Vectors. Jun 27;9:361.

[6] Zhou L, Liu Z, Wang Z, Yu S, Long T, Zhou X, Bao Y. 2017. Astragalus polysaccharides exerts immunomodulatory effects via TLR4-mediated MyD88-dependent signaling pathway in vitro and in vivo. Sci Rep. Mar 17;7:44822.

[7] Shackelford C, Long G, Wolf J, Okerberg C, Herbert R. Qualitative and Quantitative Analysis of Nonneoplastic Lesions in Toxicology Studies. Toxicologic Pathology. 2002;30(1):93-96.

[8] Suresh V, Parida D, Minz AP, Sethi M, Sahoo BS, Senapati S. Tissue Distribution of ACE2 Protein in Syrian Golden Hamster (Mesocricetus auratus) and Its Possible Implications in SARS-CoV-2 Related Studies. Front Pharmacol. 2021 Jan 14;11:579330.

[9] K-H. Chan, S. Sridhar, R.R. Zhang, H. Chu, A.Y-F. Fung, G. Chan, J.F-W. Chan, I.F-N. Hung, V.C-C. Cheng, Factors affecting stability and infectivity of SARS-CoV-2. Journal

of Hospital Infection. Front Pharmacol. 106 (2020) 226e231.

[10] Marzi A, Banadyga L, Haddock E, Thomas T, Shen K, Horne EJ, Scott DP, Feldmann H & Ebihara H (2016) A hamster model for Marburg virus infection accurately recapitulates Marburg hemorrhagic fever. Sci Rep 6: 39214.

[11] Sencio V, Machelart A, Robil C, et al. (2022) Alteration of the gut microbiota following SARS-CoV-2 infection correlates with disease severity in hamsters. Gut Microbes 14.